

Auditory Filter Behavior and Updated Estimated Constants

Journal Title
 XX(X):1–19
 ©The Author(s) 2025
 Reprints and permission:
sagepub.co.uk/journalsPermissions.nav
 DOI: 10.1177/ToBeAssigned
www.sagepub.com/

SAGE

Samiya A Alkhairy¹

Abstract

Filters from the Gammatone family are often used to model auditory signal processing, but the filter constant values used to mimic human hearing are largely set to values based on historical psychoacoustic data collected several decades ago. Here, we move away from this long-standing convention, and estimate filter constants using a range of more recent reported filter characteristics (such as quality factors and ratios between quality factors and peak group delay) within a characteristics-based framework that clarifies how filter behavior is related to the underlying constants. Using a sharp-filter approximation that captures shared peak-region behavior across certain classes of filters, we analyze the range of behaviors accessible when the full degrees of freedom of the filter are utilized rather than fixing the filter order or exponent to historically prescribed values. Filter behavior is characterized using magnitude-based and phase-based characteristics and their ratios, which reveal which characteristics are informative for constraining filter constants and which are only weakly constraining. We show that these insights and estimation methods extend to multiple realizable filter classes from the Gammatone family and apply them, together with recent physiological and psychoacoustic observations, to derive constraints on and estimates for filter constants for human auditory filters. More broadly, this framework supports the design of auditory filters with arbitrary characteristic-level specifications and enables systematic assessment of how variations in filter characteristics influence auditory models, perceptual findings, and technologies that rely on auditory filterbanks.

Keywords

auditory filterbanks, auditory filters, ERB, filter design, psychoacoustics, simultaneous masking, forward masking, tuning curves, filter characteristics, group delay, tuning ratio, parameter space, sensitivity, cochlear modeling

Introduction

Motivation

Gammatone filters and related classes of filters have typically been used to mimic auditory signal processing. The Gammatone filters used to mimic signal processing in humans have been fixed to fourth order, with a second parameter that is typically set based on equivalent rectangular bandwidths (ERBs) as described in [Slaney et al. \(1993\)](#). The chosen value of the filter order is due to fits to tuning curves from simultaneous masking psychoacoustic measurements that were performed several decades ago by [Glasberg and Moore \(1990\)](#).

This leaves us with two questions. The first is regarding understanding the full range of behavior accessible by these filters - beyond fixed order filters, and their implications on the values of filter characteristics such as peak frequencies, 3 dB quality factors, ERBs, and group delays at the peak. The second is regarding how we may design the auditory filters to account for recent information that contradicts the simultaneous masking results.

Answering the first question allows to determine whether certain types of behavior may be fulfilled by auditory filters, how these map onto requirements on filter characteristics, and the sensitivity of filter characteristics to changes in filter constants over a reasonable range of values. We propose that this analysis

is at least as important - if not more important, than constructing new classes of auditory filters and studying the difference between them.

Addressing the second question requires appropriate methods to design the filters and estimate the filter constants given tuning curves or reported values of filter characteristics. Here we choose the latter, and note that proper methods to design filter given filter characteristics must build on an analysis of the filter behavior as well as the sensitivity of the filter characteristics to filter constants. The alternative approach is to fit the filters to newly reported tuning curves, but this would again result in fixed values of filter constants without an understanding of how they are related to descriptions of filter behavior encoded in reported filter characteristics.

Goal and Objective

These two questions lead us to our goal which is to design human auditory filters given recently reported values of filter characteristics in a manner that allows us to understand how varying the filter characteristics influences the estimated filter constants. Our goal is achieved by fulfilling three objectives: (1) analyzing the behavior of filters and the dependence of filter characteristics on filter constants, (2) improving methods for estimating the filter constants from specifications on sets of filter characteristics, and (3)

¹Massachusetts Institute of Technology, USA and King Abdulaziz City for Science and Technology, KSA

Prepared using sagej.cls [Version: 2017/01/17 v1.20]

Corresponding author:

Samiya Alkhairy

estimating constraints on and values for the filter constants using recent observations and reported values for filter characteristics relevant for humans.

Our methods and estimates apply to several classes of filters from the Gammatone family. In the next section, we fulfill the first two objectives using a sharp-filter approximation for various filter classes, and in the following section, we demonstrate that our findings and methods for at least three classes of filters that are well-approximated by the sharp-filter approximation in the peak region for the parameter region of interest.

We then proceed to estimating the constraints and filter constant values for our third objective where we exemplify the use of the aforementioned characteristics-based filter design methods to estimate the values of filter constants for human auditory filterbanks given a few reported values of characteristics. In particular, we use reported values of the a ratio found to be constant in chinchilla and assumed to be the same across species [Shera et al. (2010)] and equivalent rectangular bandwidths reported from recent forward masking psychoacoustic experiments [Oxenham and Sera (2003)].

Significance

Beyond estimating filter constants for human auditory filters based on recent experiments, we present guidelines for the estimation of filter constants given various sets of reported characteristics. The intuition developed, the filter design methods, and the expressions relating filter characteristics and filter constants further allow (1) designing filters given specification of arbitrary values for the filter characteristics (e.g. personalized filters or to mimic different species), and (2) *systematically* studying the dependence of findings of perceptual studies and models as well as the performance of technologies e.g. [Dietz et al. (2011); Dimitriadis et al. (2010)] on filter characteristics.

Sharp-filter Approximation

In this section we discuss a sharp filter approximation of several realizable classes of filters that may be designed to mimic auditory signal processing in humans. This sharp-filter approximation is not realizable but its simplicity enables the analysis of its behavior and development of methods to estimate the filter constants parameterizing its transfer function from reported (or desired) values of filter characteristics. The behavior and estimation methods carry over the the realizable filters of interest as show later in this paper.

Transfer Function

Here we review the transfer function of the sharp-filter approximation of the various classes of filters. We present the continuous frequency domain expressions in normalized frequency,

$$\beta \triangleq \frac{f}{\text{CF}} \quad (1)$$

which is in terms of the frequency, f , and the characteristic frequency, CF. The time domain expressions are in scaled time,

$$\tilde{t} \triangleq 2\pi\text{CF}t. \quad (2)$$

The transfer functions are not in the Laplace domain but rather in normalized continuous complex frequency, s , where,

$$\text{Im}\{s\} = \beta. \quad (3)$$

The transfer functions are of the form,

$$H_{\text{sharp}} \propto (s - p)^{-B_u}, \quad (4)$$

where the repeated pole is $p = -A_p + ib_p$, and the exponent to the base filter transfer function is B_u . We henceforth refer to $(A_p, b_p, B_u) \in \mathbb{R}^{3+}$ as the set of filter constants parameterizing the transfer function.

We note the use of proportionality rather than equality in the above expression as well as in other expressions for transfer functions and impulse responses in this paper. We do so as we are not concerned with mapping the gain constant from the transfer function of one class of filters to its impulse response or to the transfer function of the sharp-filter approximation. We are not concerned with the variation of the gain constants across CF in a filterbank, or across different classes of filters. When plotting the frequency response, we normalize the magnitude to that at the peak - and reference the phases so that they start at zero.

The H_{sharp} was independently derived as a sharp-filter approximations for both the Generalized-Exponent Filters (GEFs/P) [Alkhairy (2025a)] and for the classical Gammatone Filters (GTFs) [Holdsworth et al. (1988); Darling (1991)]. We note that the set of filter constants (A_p, b_p, B_u) are the native parameters for the transfer functions for GEFs and V (discussed in a later section) and we re-express GTFs in these parameters so as to deal with a single parameterization for all classes of filters. The transfer function H_{sharp} is particularly good at approximating the aforementioned classes of auditory filters for small values of A_p and particularly in the region of the peak as shown in figure 1.

While this class of filters is itself not realizable, the simplicity of its transfer function enables us to derive closed-form expressions for (primarily peak-centric) filter characteristics - e.g. 3dB quality factor, in terms of filter constants. These expressions form the basis upon which we develop our methods to estimate filter constants from reported values of filter characteristics. Over the course of the next few sections, we return to these fundamental expressions, derive expressions for various filter characteristics (including characteristic ratios), study the dependence of the filter characteristics on the pole and filter exponent, and develop accurate methods for the design of filters given values of characteristics, and provide estimates for the filter constants given reported observations and values for filter characteristics.

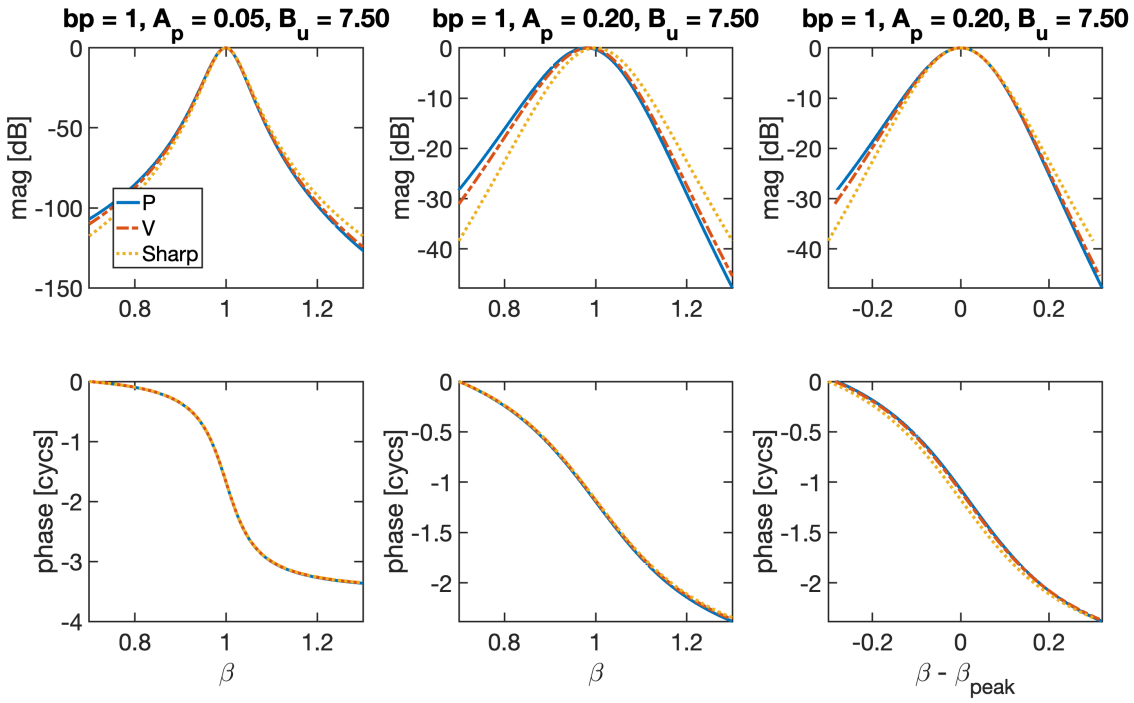


Figure 1. The left and middle panels show the Bode plots as a function of normalized frequency, β , for the following transfer functions: H_P (blue solid lines), H_V (red dash-dotted lines), and the approximation, H_{sharp} (yellow dotted lines), which we use to derive our expressions for filter characteristics in terms of filter constants and based upon which the characteristics-based filter design methods are developed. The left and middle panels are generated using two different sets of filter constant values (shown in the panel titles) chosen from the range we deem appropriate in humans. The left panel is more appropriate for filters with larger CFs and the middle panel is for lower CFs. The left and middle shows that H_{sharp} is a good approximation for the transfer functions for the realizable filters, H_P and H_V . In the rightmost panel, we show the validity of this approximation more clearly for the transfer functions from the middle panel by shifting the x axis by β_{peak} , which takes on the following values for each of the curves: $\beta_{\text{peak},P} = 0.9798$, $\beta_{\text{peak},V} = 0.9852$, and $\beta_{\text{peak, Sharp}} = 1$.

Dependence of Filter Behavior on Constants

In this section, we show the rich array of possible filter behavior - quantified via filter characteristics, that we can attain provided that we allow ourselves to access the range of values for all degrees of freedom - A_p, B_u, b_p , rather than restrict ourselves to certain values of B_u as has typically been the case. We discuss the dependence of filter characteristics on filter constants in order to build intuition about the filters, infer constraints on filter constants given observations, and as the first step towards developing methods to estimate filter constants given specifications on filter characteristics. We perform this analysis here for H_{sharp} which approximates the common features across realizable classes of filters from the Gammatone family of filters. In a later section, we demonstrate the validity of our findings for realizable filters.

Expressions for Filter Characteristics We limit ourselves to certain frequency domain characteristics and do not include asymmetry of the magnitude of the frequency response which is fundamentally different across the realizable classes of filters in the Gammatone family of filters. We define the filter characteristics in the normalized frequency (β) domain and express them in terms of the set of filter constants (A_p, b_p, B_u) that parameterizes the transfer function. Using the expression for H_{sharp} (equation 4), we derive the following expressions for filter characteristics as

functions of the filter constants. These include both magnitude-based characteristics ($\beta_{\text{peak}}, Q_n, Q_{\text{erb}}, S_\beta$) and phase-based characteristics ($\beta_{\text{maxN}}, N_\beta, \phi_{\text{accum}}$).

$$\begin{aligned}
 \beta_{\text{peak}} &= b_p \\
 Q_n &= \frac{b_p}{2A_p} \left(10^{\frac{n}{10B_u}} - 1 \right)^{-\frac{1}{2}} \\
 Q_{\text{erb}} &= \frac{b_p}{\sqrt{\pi} A_p} \frac{\Gamma(B_u)}{\Gamma(B_u - \frac{1}{2})} \\
 S_\beta &= \frac{20}{\log(10)} \frac{B_u}{A_p^2} \\
 \beta_{\text{maxN}} &= b_p \\
 N_\beta &= \frac{1}{2\pi} \frac{B_u}{A_p} \\
 \phi_{\text{accum}} &= \frac{B_u}{2}
 \end{aligned} \tag{5}$$

We derive our expression for Q_{erb} in the appendix of this paper. The derivation for most of the other characteristics was previously detailed in Alkhairy (2025a).

Variation of Characteristics with Constants In what follows, we describe how the magnitude-based and phase-based filter characteristics of H_{sharp} vary with the filter constants as may be guided by the closed-form expressions in equation 5. These descriptions also hold

for the realizable classes of auditory filters discussed later.

The first of the magnitude-based characteristics - the peak normalized frequency, β_{peak} , of H_{sharp} depends only on b_p which we typically assign to unity. However, we may choose to vary the value of b_p if we are interested in designing filters for which the peak frequency (best frequency), $f_{peak} = b_p \text{CF}$, is not simply equal to the characteristic frequency. For instance, one may choose to set $b_p < 1$ so that $f_{peak} < \text{CF}$ (e.g. to account for filter behavior at higher SPLs without fully moving to nonlinear filters).

The two quality factors in equation 5 - the quality factor based on an n dB bandwidth, Q_n , and the quality factor based on the equivalent rectangular bandwidth (ERB), Q_{erb} - are both proportional to b_p and inversely proportional to A_p . The quality factors also increase with the filter exponent B_u but in a more complicated manner. The n dB quality factor is naturally smaller for larger n - e.g. $Q_{15} < Q_3$.

The last magnitude-based filter characteristic in equation 5 is the degree of downward convexity at the peak frequency, S_β , in dB. This filter characteristic was introduced in Alkhairy (2025a) as the most peak-centric of the magnitude-based filter characteristic as it only depends on the second derivative of the magnitude (in dB) at β_{peak} . Similar to the bandwidths that are defined in the β domain, ERB_β and BW_n , the convexity measure, S_β , is a measure of the sharpness of tuning. It is independent of b_p (like ERB_β and BW_n but unlike Q_{erb} and Q_n), is inversely proportional to A_p^2 and hence highly sensitive to it, and is simply linearly proportional to B_u , rendering it the simplest of the measures for sharpness of tuning. For experimental data, its use is limited by sampling rate and SNR, but it is quite appropriate for models, filters, finely sampled data at high SNR, and fitted data - e.g. Tan and Carney (2003).

As for the phase-based characteristics: the maximum group delay occurs at β_{maxN} which in the case of H_{sharp} occurs at β_{peak} . However, in the case of the realizable filters, they are similar to one another but are not exactly equal as may be inferred from figure 1.

The maximum group delay or equivalently (for H_{sharp}) the group delay at the peak, N_β , in cycles, is linearly proportional to B_u and inversely proportional to A_p . The phase accumulation, ϕ_{accum} in cycles, is solely dependent on - and directly proportional to, the filter exponent B_u . As expected, if $B_u = 1$ - i.e. we have a second order filter describing a damped harmonic oscillator, the phase accumulation is half a cycle.

These observations regarding the dependence of filter characteristics of H_{sharp} are visualized in figure 2. These plots also may serve as a 'look-up' table of sorts for those who design filters by specifying values of filter constants to fulfill certain specifications on filter characteristics. In the figure, we have set $b_p = 1$ (i.e. $f_{peak} = \text{CF}$) for simplicity. We bounded the domain of filter constants to include range - that we find later in the paper, to be most appropriate for filterbanks mimicking auditory signal processing in humans.

Dependence of Characteristic Ratios on Filter Constants

One particular type of filter characteristics is defined as combinations of some of the filter characteristics mentioned above. It is relevant to discuss the dependence of these combined characteristics on filter constants as we later used them to estimate filter constants.

This is motivated by reports from recent work of CF-invariant and/or species-invariant values or patterns in ratios of some of the aforementioned characteristics - e.g. $\frac{Q_{erb}}{N_\beta}$ across CF in chinchilla, and $\frac{Q_{erb}}{Q_{10}}$ across species and CF [Shera and Guinan Jr (2003); Sera et al. (2010)]. In what follows, we study the dependence of such characteristic ratios on the filter constants. We limit our interest to characteristic ratios that depend only on B_u or only on A_p and which we can derive using expressions in equation 5.

Of particular interest are α and g which we may express based on the sharp-filter expressions in equation 5 as follows. In a later section, we use reported values for the above characteristic ratios to provide bounds or estimates for filter constants.

$$\begin{aligned} \alpha &\triangleq \frac{Q_{erb}}{Q_{10}} = \frac{2}{\sqrt{\pi}} \frac{\Gamma(B_u)}{\Gamma(B_u - \frac{1}{2})} \sqrt{10^{1/B_u} - 1} \\ g &\triangleq \frac{Q_{erb}}{N_\beta} = 2\sqrt{\pi} b_p \frac{\Gamma(B_u)}{B_u \Gamma(B_u - \frac{1}{2})}. \end{aligned} \quad (6)$$

In figure 3a, we plot a subset of the following ratios of filter characteristics for H_{sharp} that may be expressed (when using equation 5) purely as functions of the filter exponent B_u :

- $\frac{Q_{erb}}{Q_n} \equiv \frac{\text{BW}_{n,\beta}}{\text{ERB}_\beta}, \frac{Q_n}{Q_m} \equiv \frac{\text{BW}_{m,\beta}}{\text{BW}_{n,\beta}}$ which are dimensionless
- $\frac{Q_{erb}^2}{\beta_{peak}^2 S_\beta} \equiv (\text{ERB}_\beta^2 S_\beta)^{-1}, \frac{Q_n^2}{\beta_{peak}^2 S_\beta} \equiv (\text{BW}_{n,\beta}^2 S_\beta)^{-1}$ in dB⁻¹
- $\frac{Q_{erb}}{\beta_{peak} N_\beta} \equiv (\text{ERB}_\beta N_\beta)^{-1}, \frac{Q_n}{\beta_{peak} N_\beta} \equiv (\text{BW}_{n,\beta} N_\beta)^{-1}$ in cycs⁻¹

Reported values for ratios that strongly depend on B_u may be used to estimate B_u . However, ratios that weakly vary with B_u over the range of interest such as α cannot be used to determine B_u - but can be used to estimate bounds for B_u with some degree of confidence (as done later in this paper). The same is true for $\frac{g}{b_p}$ at larger values of B_u .

In figure 3b, we plot the ratios $\frac{S_\beta}{N_\beta}$ (in dB/cy whole) and $\frac{\phi_{accum}}{N_\beta}$ (which is dimensionless) which we derived using equation 5 and are purely functions of A_p . These ratios are strongly dependent on A_p and hence if we obtain reported values for either of these ratios, we can determine the value of A_p .

Use of Expressions In this section, we have studied the dependence of filter characteristics (including characteristic ratios) on filter constants. The filter characteristics discussed here are common among the three classes of realizable filters discussed in this paper and the our findings apply to these classes as shown in a later section. Characteristics that are

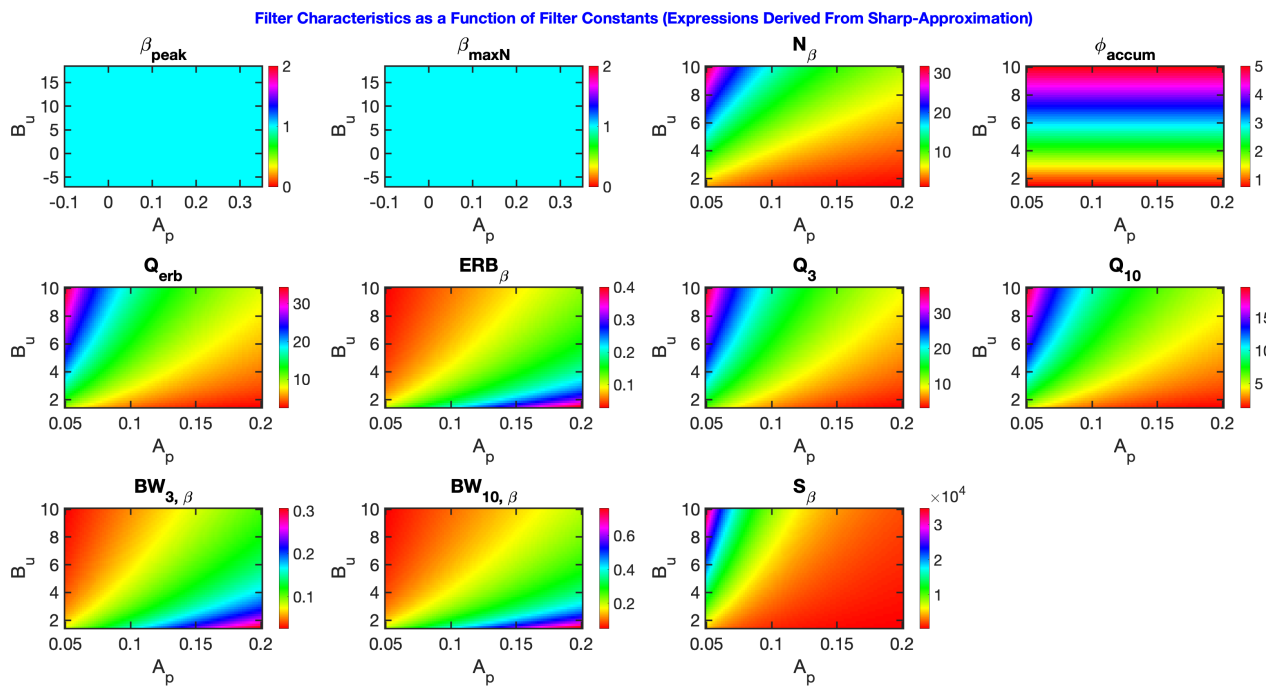


Figure 2. We plot various filter characteristics of H_{sharp} as a function of filter constants A_p and B_u using the closed-form expressions in equation 5. For the quality factors, β_{peak} and β_{maxN} , which depend on b_p , we used $b_p = 1$ (i.e. $f_{\text{peak}} = \text{CF}$). These plots (along with plots of the characteristic ratios in figure 3) may be used to understand the effects of varying the filter exponent and pole on behavior, to understand the relationship between various characteristics, and as a look-up table to quickly estimate filter constants or serve as a stepping stone by providing initial guesses for the characteristics-based filter design methods.

inherently different across the classes of filters such as the asymmetry of the power spectrum are not discussed in this paper.

We have shown a wide range of filter characteristics accessible when fully availing the degrees of freedom of a given filter class. The full range of behavior shown in figure 2 should encourage us to prioritize proper estimation of filter constants over choosing a filter class with a particular type of off-peak behavior. We also derived expressions for characteristic ratios which we later use to determine constraints on filter constant values (particularly B_u) and to inform the methods by which we estimate constants given reported values of filter characteristics.

The observations we made in this section have direct implications for characteristics-based estimation of filter constants: We note that (non-ratio) characteristics must be used in combinations to estimate the filter constants. For instance, reported bandwidth-based characteristics depend on both the pole and filter exponent, and their use alone to estimate the filter constants would lead to a ill-posed inverse problem in which small changes in the B_u can be compensated by changes in the A_p . In contrast, this identifiability issue does not arise when using characteristic ratios alone that depend primarily on a single filter constant.

Methods for Estimating Filter Constants from Characteristics

Our goal is to estimate filter constants for auditory filters mimicking human signal processing based

on recent reported values of filter characteristics and characteristic ratios. This requires developing accurate methods for estimating filter constants given specifications on filter characteristics. In this section, we discuss the appropriate choices for the set of filter characteristics used for this estimation. We then present methods for accurate characteristic-based filter constant-estimation and filter design, and finally compare the proposed methods with existing characteristics-based methods.

Sets of Filter Characteristics Used The choice of characteristics used to estimate b_p is straightforward - are typically provided with β_{peak} and CF from which we may estimate the value of b_p . However, it is important to discuss the characteristics used to estimating the remaining filter constants, A_p and B_u .

The particular choices of characteristics and/or characteristic ratios used for estimating the filter constants depend not only on the availability of reported values, but also on the needs of a particular study or application. For instance, if we are interested in designing filters that are sharply tuned but have a limited group delay, it is natural to simultaneously specify a mixed set of two characteristics - one on a magnitude-based characteristic, and the other on a phase-based characteristic (e.g ERB and N_β) or an equivalent set of characteristic and characteristic-ratio (e.g. Q_{erb} and g or S_β and $\frac{S_\beta}{N_\beta}$). Similarly, we would choose to use such mixed-type specifications if we are interested in dictating the frequency selectivity and synchronization across filters in a filter bank.

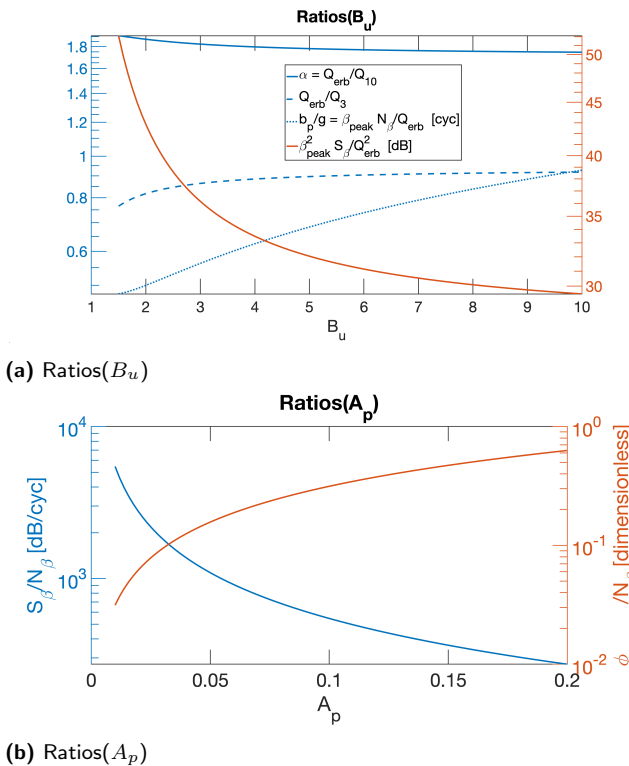


Figure 3. We plot the dependence of several filter characteristics ratios that depend solely on a single filter constant - A_p or B_u , as derived using the expressions from equation 5 based on H_{sharp} . The top panel reveals that certain B_u -dependent ratios such as $\frac{Q_{\text{erb}}}{Q_{10}}$ are not particularly useful for determining specific values of B_u due to their slow variation with respect to B_u in the parameter region of interest. We note that for larger values of B_u , $\frac{g}{b_p}$ and $\frac{Q_{\text{erb}}^2}{\beta_{\text{peak}}^2 S_{\beta}}$ also exhibit shallow dependence. In contrast, both ratios that are purely functions of A_p - i.e. $\frac{S_{\beta}}{N_{\beta}}$ and $\frac{\phi_{\text{accum}}}{N_{\beta}}$, exhibit a strong dependence on A_p and hence - when available, may reliably be used to determine this filter constant.

Alternatively, if the application or study of interest requires fine control over the magnitude of the frequency response, then it is appropriate to simultaneously specify a set of two magnitude-based filter characteristics (e.g. S_{β} and Q_{erb}) or an equivalent set of filter characteristic and characteristic ratio which are then used to estimate the filter constants. We suggest avoiding the combined set of Q_{erb} and Q_{10} or alternatively, one of these two characteristics along with the ratio α . This is due to the fact that α varies slowly with B_u - or equivalently, $|\frac{dB_u}{d\alpha}|$ is very large, over the region of interest (see figure 3a), and hence these sets are not appropriate for reliably estimating filter constants.

If we are designing filters to mimic auditory signal processing (as is the case here) rather than to fulfill arbitrary specifications on characteristics, we avoid the use of the ϕ_{accum} characteristic to estimate B_u . This is due to the fact that the filter classes were all constructed based on the shape of tuning curves. However, these curves are only measured in the region near the peak which is what predominantly influences the results of signal processing. Consequently, while the filter classes may be used to mimic auditory signal processing of a

particular species, it is inappropriate to suggest that the off-peak behavior of these filters (including ϕ_{accum}) mimics that of the actual auditory system.

Proposed Method Once we have chosen the set of characteristics to use, we proceed to the filter constant estimation method. Rather than simultaneously solving for the filter constants, we first start by estimating b_p , followed by B_u , and finally, A_p .

As mentioned above, we may estimate the value of b_p from β_{peak} . Alternatively, if we are only concerned with a single level, we may simply set $b_p = 1$. We may then estimate B_u using reported (or computed) ratios of filter characteristics that depend solely on B_u . Characteristic ratios or combinations such as $\text{ERB}_{\beta} N_{\beta}$, $\text{BW}_{3,\beta} N_{\beta}$, $\text{ERB}_{\beta}^2 S_{\beta}$, $\text{BW}_{3,\beta}^2 S_{\beta}$ are preferable to characteristic ratios such as $\frac{\text{BW}_{3,\beta}}{\text{ERB}_{\beta}}$ or $\frac{\text{BW}_{3,\beta}}{\text{BW}_{10,\beta}}$ as the latter set is not particularly sensitive to variations in B_u over the parameter region of interest and hence we cannot obtain reliable estimates of B_u from these. After being provided with (or computing) B_u -dependent characteristic ratios, we solve the nonlinear equation in the characteristic ratio (based on equation equation 5) to estimate B_u .

We then use the estimates of B_u and b_p , along with the value of one of the reported characteristics (e.g. Q_{erb}), and the expression for the corresponding filter characteristic in equation 5 to solve for A_p . This is a simple linear equation that is directly solved for A_p . We return to these methods and make use of them in later sections to estimate the filter constants from recent reported filter characteristics.

We note that instead of estimating B_u followed by A_p , we may do the opposite - after estimating b_p we may first estimate A_p using the expressions for one of the A_p -dependent characteristic ratios (e.g. $\frac{S_{\beta}}{N_{\beta}}$, $\frac{\phi_{\text{accum}}}{N_{\beta}}$) and then estimate B_u . However, as previously mentioned, we avoid using designing filters based on ϕ_{accum} , and note that S_{β} are currently not reported.

Comparison with Existing Methods The aforementioned methods of estimating the values of the b_p then solving a nonlinear equation for B_u then a linear equation for A_p allows us to design filters given reported characteristics more accurately (if using Q_{erb}) than previously developed characteristic-based filter design methods [Alkhairy (2025a)]. Previous methods involved the derivation and use of explicit expressions for each filter constants in terms of desired filter characteristics. This extra step made the constant estimation problem (and filter design methods) far more direct and did not require solving a nonlinear equation (when using Q_{erb}). However, it required making an additional approximation for the case of Q_{erb} beyond that of the sharp-filter approximation - which allowed us to express $\log(\text{ERB}_{\beta})$ as a linear combination of $\log(A_p)$, $\log(B_u)$. This in turn reduced the accuracy of the method compared to the methods presented in this section which require no additional approximations beyond the sharp-filter approximation used to derive equation 5.

As a result, if we are interested in designing auditory filters with increased accuracy, we suggest using the methods outlined above. At the step involving solving the nonlinear equation for B_u , we may provide an initial estimate for B_u based on the previous direct methods for filter constant estimation, or simply by using figure 2 and 3a as look-up tables to find the initial estimates.

Alternatively, if we are interested in systematically and semi-analytically studying the dependence of findings of perceptual models or technological contributions on filter characteristics, it may be more appropriate to deal with the previously derived methods which provided explicit expressions for filter constants (and hence any function of these filter constants deemed useful for these studies) directly in terms of filter characteristics.

Realizable Filters

This section establishes that the characteristic-constant relationships and methods derived in the previous section are not artifacts of a particular class, but apply broadly across commonly used gammatone-family filters. In the previous section, we worked with the transfer function H_{sharp} which approximates the transfer function of several realizable filter classes of the Gammatone family of filters. We first reviewed the expressions for H_{sharp} in the normalized frequency domain parameterized by filter constants. We then presented expressions for the filter characteristics of H_{sharp} in terms of filter constants, analyzed the behavior of these filters and the sensitivity of their filter characteristics to changes filter constants in the parameter region of interest, and developed methods to design the filters (i.e. estimate the filter constants) given arbitrary specifications on filter characteristics. The filter with H_{sharp} is itself is unrealizable but it approximates several classes of realizable filters in the peak region when A_p is small - as is the case for filters mimicking processing in humans.

In this section, we focus on the classes of realizable filters which have a transfer function that may be approximated by H_{sharp} in the peak region. We first review these classes of filters and show that they are all parameterized by the same set of filter constants. We then demonstrate that the behavior and dependence of peak-centric characteristics describing these realizable classes of filters carry over from those obtained for the filter with H_{sharp} . Consequently, if we use peak-centric characteristics to estimate the filter constant, we only need to do so once regardless of filter class. Note that we are not interested in characteristics that differ across classes such as asymmetry or characteristics related to the magnitude at the peak.

Classes of Realizable Filters

The classes of realizable filters that we study here are: the Generalized Exponent Filter (GEFs/P filters), the V filter, and the classical Gammatone filter (GTFs). These are tightly related to the All Pole Gammatone Filter (APGF) and the One Zero Gammatone Filter (OZGF), as well as the Q filter and Differentiated All Pole

Gammatone Filter (DAPGF) as described in Table 1. Consequently, we expect that our conclusions regarding the applicability of our conclusions and methods for H_{sharp} not only applies to GEFs/P, V, and GTFs, but also to the other classes of filters in the table.

Generalized-Exponent (P) Filters The first class of realizable filters for which our conclusions from H_{sharp} apply is the Generalized-Exponent (or P) class of filters which have a transfer function,

$$H_P(s; A_p, b_p, B_u) \propto \left((s - p)(s - \bar{p}) \right)^{-B_u}. \quad (7)$$

In separate work, we had shown that GEFs with rational values of the exponent, B_u may be implemented in software and used to process signals [Alkhairy (2025b)]. As a result, we need not restrict ourselves to integer values of B_u .

In figure 1, we show the frequency response magnitude and phase for GEFs (blue solid lines) and the sharp-filter approximation (dotted yellow lines) for a few different sets of filter constant values of interest. The figure shows that the bandwidth of H_P is well approximated by that of H_{sharp} - particularly when we plot the frequency response magnitude as a function of $\beta - \beta_{\text{peak}}$.

The GEFs have an impulse response which we express in $\tilde{t} = 2\pi CFT$, and which may be expressed for integer and half-integer values of B_u as follows,

$$g_P \propto e^{-A_p \tilde{t}} \tilde{t}^{B_u - \frac{1}{2}} J_{B_u - \frac{1}{2}}(b_p \tilde{t}) u(\tilde{t}) \quad \text{for } B_u \in \frac{\mathbb{Z}^+}{2}, \quad (8)$$

where $u(\tilde{t})$ is the Heaviside step function and where $J_{B_u - \frac{1}{2}}(b_p \tilde{t})$ is a Bessel function of the first kind.

We may approximate the impulse response (for $\tilde{t} \geq 0$) by the term,

$$g_P \approx e^{-A_p \tilde{t}} \tilde{t}^{B_u - 1} \cos(b_p \tilde{t} - B_u \frac{\pi}{2}) \quad \text{for } B_u \in \frac{\mathbb{Z}^+}{2}, \quad (9)$$

as discussed in Alkhairy (2025b). This form resembles GammaTone Filters (GTFs) but the oscillatory component has a phase shift that is tied to the filter exponent B_u , and we have expanded the domain of B_u beyond positive integers. We refer to this version of GTFs as P-GTFs to distinguish it from the classical GTFs with an additional degree of freedom for the phase shift. As noted by Darling (1991), the choice of phase shift has negligible effect on the power spectrum.

We note that the transfer function of GEFs/P is essentially the same as that of APGFs but without imposing that B_u is an integer. Consequently, any conclusions we make regarding the applicability of findings and methods from H_{sharp} to H_P also applies to H_{APGF} . The reasons we directly work with (the notation of) GEFs/P here rather than the more commonly known APGFs is as follows:

- The GEFs/P filters do not require that the filter exponent, B_u be an integer. This allows us to access a broader range of filter behaviors and more finely tune the filter based on desired values for filter characteristics.

Summarizing Reference	(Repeated) pole-pair	With zero I	With zero(s) II
Alkhairy (2025a)	GEFs/P <ul style="list-style-type: none"> • Rational exponent • Related to differential pressure in cochlear model 	V <ul style="list-style-type: none"> • Rational exponent • Related to velocity in cochlear model (if parameterized by $B_u + 1$) • Zero is equal to the negative of the real part of the pole 	Q and generalized-Q <ul style="list-style-type: none"> • Rational exponent • Q has a repeated zero at zero • Generalized-Q has a repeated arbitrary zero that is far from the peak
Katsiamis et al. (2007)	APGF <ul style="list-style-type: none"> • Integer exponent • Hardware (not only software) implementations 	OZGF <ul style="list-style-type: none"> • Integer exponent • Arbitrary zero introduces an additional degree of freedom • Hardware (not only software) implementations 	DAPGF <ul style="list-style-type: none"> • Integer exponent • Has a single zero at zero • Hardware (not only software) implementations

Table 1. Description of various classes of realizable auditory filters of the gammatone family which behave the same at the peak and for which we may estimate filter constants using the filter design methods derived for H_{sharp} that are based on peak-centric filter characteristics

- The accuracy of previous characteristics-based filter design methods was assessed for GEFs.
- GEFs/P filters have origins in a unified model and can be used both as auditory filters and also as part of a cochlear model to understand the mechanisms underlying a single partition box model of the cochlea (where GEF/P filters are related to the pressure difference across the Organ of Corti in the model). Consequently, having methods to design these filters given specifications on filter characteristics also allows us to study the dependence of the related cochlear model mechanisms on the observed characteristics as described in Alkhairy (2024).

V Filters Another class of filters for which the transfer function may be approximated by H_{sharp} - and which therefore may also be designed using the same set of methods developed for characteristics-based filter design, is the V class of filters which has a transfer function,

$$H_V(s; A_p, b_p, B_u) \propto (s + A_p) \left((s - p)(s - \bar{p}) \right)^{-B_u}. \quad (10)$$

As seen in figure 1, GEFs and V filters exhibit different off-peak behavior (particularly the asymmetry of the magnitude about the peak) but are quite similar in the peak region, and the transfer function for both may be approximated by H_{sharp} .

We note that V filters are similar to OZGFs but with one less degree of freedom. Consequently, any conclusions we make regarding the applicability of findings and methods from H_{sharp} to H_V also applies to H_{OZGF} in aspects where the effect of the position zero is negligible. We make the choice of describing V rather than OZGFs here for the following reasons,

- Unlike OZGFs, it has the same degrees of freedom as H_{sharp}
- Like GEFs, V filters are not required to have integer exponents
- Like GEFs, V filters are associated with a unified cochlear model - V is related to the upward velocity, \mathcal{V} , of the OoC partition at a particular location or CF as follows (noting the difference in exponent)

$$\mathcal{V}_{\text{CF}}(s; A_p, b_p, B_u) \propto H_V(s; A_p, b_p, B_u + 1). \quad (11)$$

Gammatone Filters Our conclusions from the sharp-filter approximation also extend to the classical Gammatone filters (GTFs) [Holdsworth et al. (1988)]. This is most commonly used auditory filter, and has an impulse response typically expressed as,

$$h_{\text{GTF}} \propto t^{n-1} e^{-2\pi b t} \cos(2\pi f_c t + \phi) u(t), \quad (12)$$

where f_c is the tonal frequency, n is referred to as the filter order (classically imposed to be a positive integer), and b is often referred to as the bandwidth parameter. This may potentially be misleading as both b and n may be used to control the bandwidth. However, this terminology arose due to the fact that n was typically held constant.

The above impulse response may be expressed in \tilde{t} and parameterized by the same set of filter constants as those parameterizing H_{sharp} , H_P , and H_V , if we use the following mapping,

$$\begin{aligned} f_c &= b_p \text{CF} \\ n &= B_u \\ b &= A_p \text{CF}. \end{aligned} \quad (13)$$

We note that when comparing the impulse response of the GTF approximation of integer and half-integer

GEFs (P-GTFs) - equation 9 with the impulse response of classical GTFs - equation 12, and imposing $\phi = -\frac{\pi}{2}B_u$, we find that the two are equivalent. GTFs are the most commonly used type of auditory filter making it an obvious candidate for inclusion in this paper. The GTFs have been used in a wide range of fields, including studies and applications beyond those traditionally related to auditory signals and systems - e.g. Valero and Alias (2012); Jin et al. (2017); Matsumoto et al. (2011). Even in such applications, the values of the filter constants used are typically those historical ones used for human auditory filterbanks.

We next investigate the applicability of our findings and the suitability of the characteristics-based filter design methods developed based on the sharp-filter approximation for the cases of GEFs, V, and GTFs. The transfer functions of the aforementioned classes of filters are particularly similar in the region of the peak which is where most of the power is. This is particularly true for small A_p - i.e. when the sharp-filter approximation holds. Consequently, we expect that our conclusions from H_{sharp} carry over to these classes of filters. We also expect our conclusions to directly carry over to APGFs which is the same as GEFs. The conclusions also apply to filter classes that have different slopes and symmetries of the magnitude such as OZGFs, DAPGFs, and Q filters but only for specific ranges values of filter constants such that there is negligible effect on the peak region (e.g. the zero is far away enough from the peak).

Behavior and Filter Design for Realizable Filters

In previous sections, we discussed the range of possible behaviors and methods for estimating the filter constants for H_{sharp} . However, our goal is the study of behavior and estimating filter constants for the realizable classes of auditory filters. Therefore, it is necessary to demonstrate that our findings and methods for H_{sharp} also apply for the realizable classes of filters. We focus on the errors in the filter characteristics for each of the realizable filters as a function of the filter constants. There is no need to also discuss the errors in the filter design method as they apply to realizable filters as there are no additional approximations between these expressions needed to estimate the filter constants from the filter characteristics.

Applicability for GEFs/P We first discuss the validity of the findings (equation 5) as they apply to the case of GEFs. Over a range of filter constants where A_p is small - including the region we expect to be most appropriate for filterbanks mimicking auditory signal processing in humans, H_{sharp} is a good approximation of H_P as seen in figure 1.

The approximation of the phase of H_P by $\text{phase}\{H_{\text{sharp}}\}$ is more accurate than the approximation of the $\text{mag}\{H_P\}$ by $\text{mag}\{H_{\text{sharp}}\}$ as may also be seen from figure 1. Consequently, our closed-form expressions (equation 5) for phase-based characteristics such as N_β and ϕ_{accum} are generally more accurate than our expressions for magnitude-based filter characteristics

such as Q_{erb} and Q_n - though the expressions for bandwidths are more accurate than the quality factors which are affected due to the errors in β_{peak} . Expressions for measures of sharpness of tuning that are more peak-centric are more accurate than those that relate to bandwidths for larger n .

Upon numerically computing the relevant characteristic ratios from the frequency response of H_P , we find that the ratios are indeed approximately univariate in either A_p or B_u for the range of A_p and B_u of primary interest. We also find that, quantitatively, the numerically computed ratios are well-approximated by those in figure 3 and our closed-form expressions in equation 5.

We demonstrate the accuracy of expressions for characteristics in terms of constants for the case of GEFs/P in figure 4 which shows the relative error in a set of filter characteristics as a function of the filter constants A_p and B_u (while fixing $b_p = 1$). We define the relative error in a particular filter characteristic, γ , at some value of $(A_p, B_u, b_p = 1)$ as the deviation from unity of the ratio of $\gamma_{\text{num-P}}$ to γ_{analytic} where $\gamma_{\text{num-P}}$ is the the value of γ obtained numerically from the frequency response of GEFs that were designed with the specified values of filter constants, and γ_{analytic} is the value of γ obtained based on the sharp-filter expressions (equation 5) using the same specified values of filter constants. We do not take the absolute value in order to determine when we are consistently over- or under-estimating certain filter characteristics. For instance, the error in Q_{erb} is defined to be $\varepsilon_{Q_{\text{erb}},P} \triangleq 1 - \frac{Q_{\text{erb},\text{num-P}}}{Q_{\text{erb},\text{analytic}}}$. The resultant relative errors shown in figure 4 demonstrate the appropriateness of using the expressions of equation 5 for determining the behavior of GEFs and estimating their filter constants from specifications on filter characteristics.

Applicability for V and P-GTFs We also show the relative errors in two of the other classes of realizable filters, V and P - GTFs (GTFs with $\phi = -B_u \frac{\pi}{2}$) *, in figures 5 and 6 respectively.

In figure 5, we show that the relative error in various filter characteristics for the case of H_V is small - particularly for smaller values of A_p as required for the validity of the sharp-filter approximation assumption. The transfer function for V has a zero at $-A_p$ (with an A_p that is particularly small for humans). Therefore, when compared with H_P , the symmetry of the magnitude of H_V is in fact closer to that of H_{sharp} . Consequently, while we had derived H_{sharp} as an approximation of H_P , the derived expressions for filter characteristics as a function of filter constants are in fact generally more accurate for H_V than they are for H_P .

In figure 6 we show the relative errors in certain filter characteristics for the case of P-GTFs . Previous work had derived H_{sharp} as an approximate transfer function for h_{GTF} when the sharp-filter approximation holds [Holdsworth et al. (1988); Darling (1991)]. Indeed, we find that the errors in figure 6 are small over the parameter region of interest.

*As previously mentioned, Darling (1991) has shown that the value of the phase shift has negligible effect on the frequency response magnitude

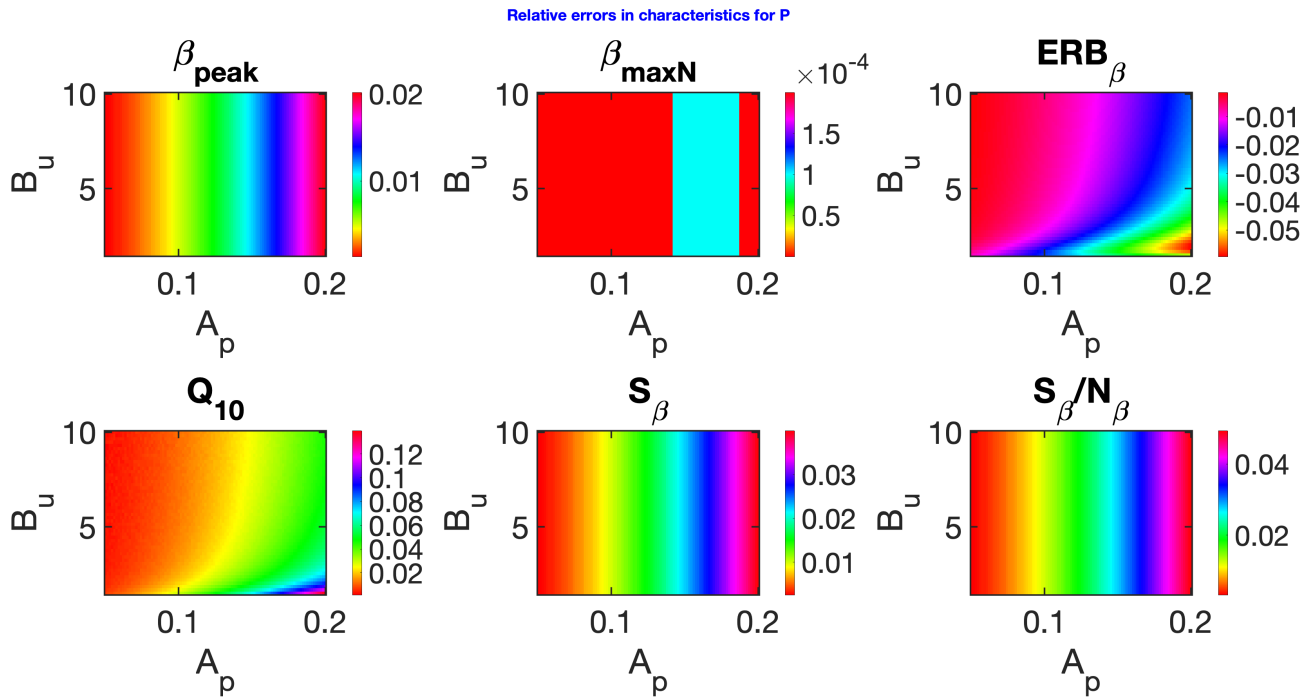


Figure 4. We show the relative errors (as a function of filter constants A_p and B_u with a fixed $b_p = 1$) of the values filter characteristics obtained using our closed-form expressions (that are based on the sharp-filter approximation) compared to those computed numerically from H_P . The relative errors are small as may be inferred from the colorbars, indicating the accuracy - for the case of GEFs, of our expressions for filter characteristics in terms of filter constants, and consequently, the accuracy of filter design methods that depend on it. The errors typically increase with A_p - i.e. as the sharp-filter approximation starts to break down.

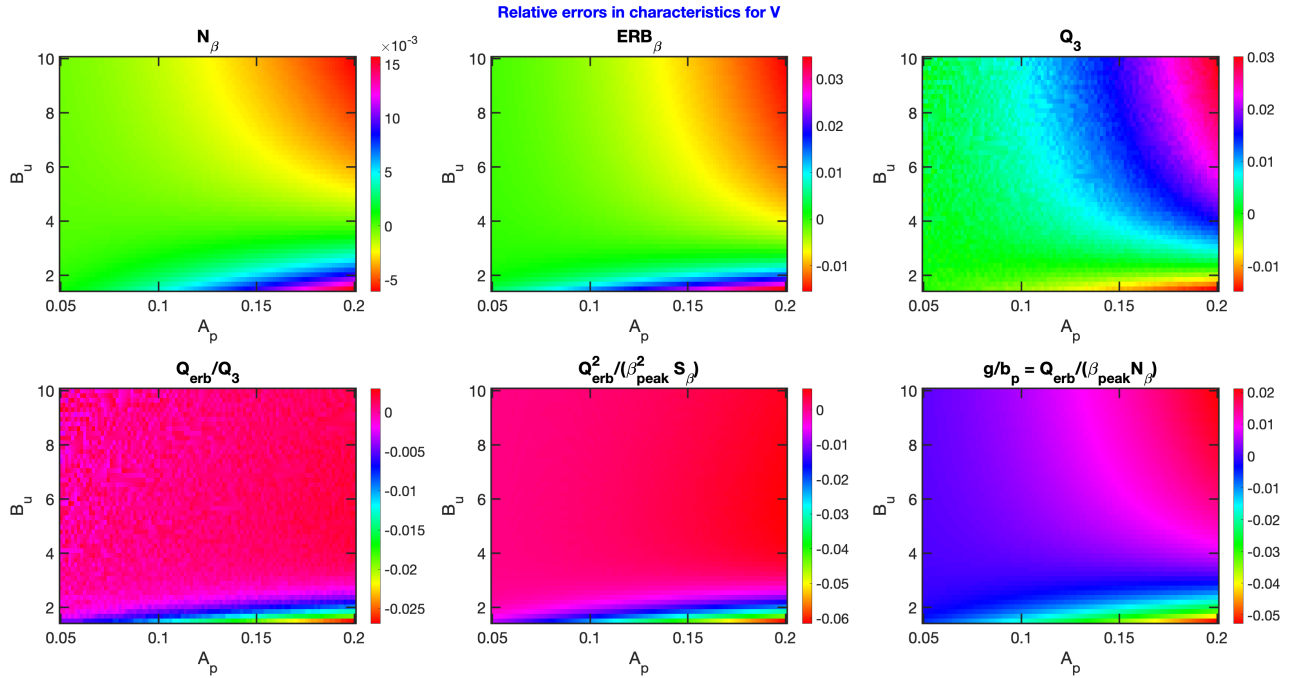


Figure 5. Relative errors in filter characteristics are small for the case of V filters as seen from the colorbars, indicating the accuracy of our expressions and methods for this class of filters.

Constraints and Estimates for Filter Exponent

In previous sections, we studied the dependence of filter characteristics on filter constants which is integral to determining which filter characteristics may reliably be

used to estimate filter constants. We also presented methods to estimate filter constants from sets of filter characteristics.

In this section, we take one step further towards estimating filter constants by deriving constraints on,

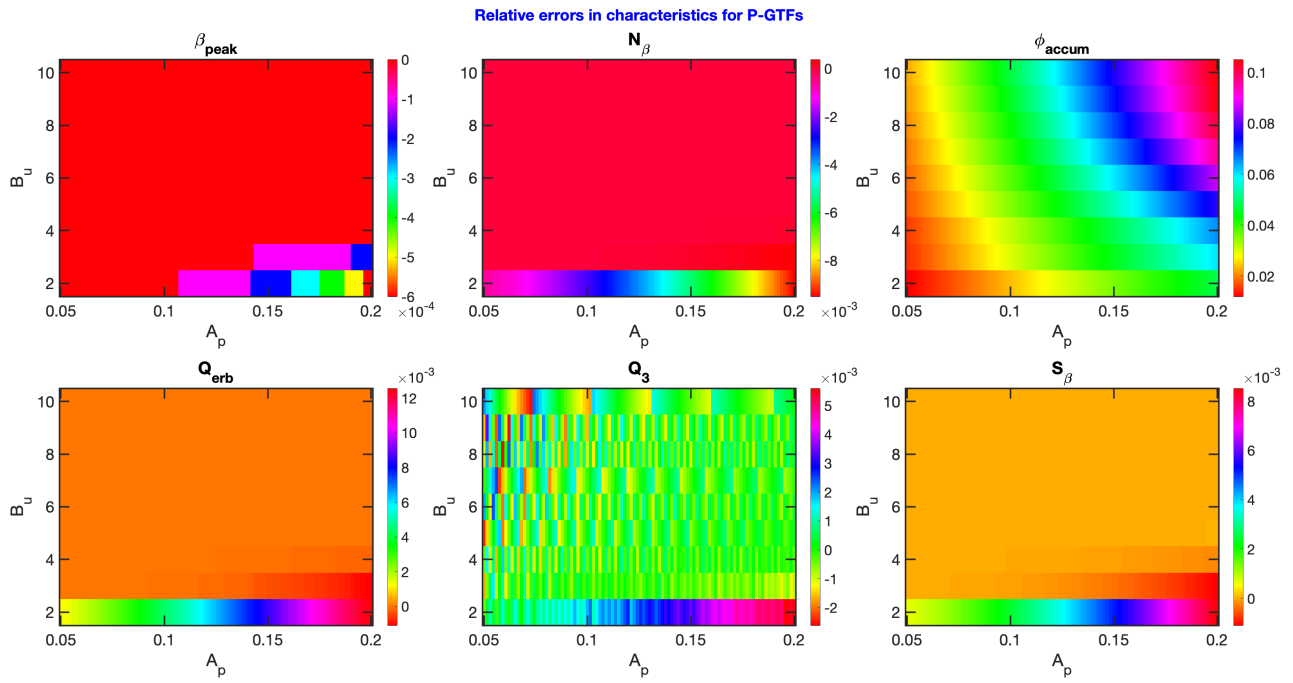


Figure 6. Relative errors in filter characteristics are small for the case of P-GTFs (GTFs with a phase shift of $-B_u \frac{\pi}{2}$ which is derived based on the approximation of the impulse response of GEFs except at the lowest times) as seen from the colorbars, indicating the accuracy of our expressions and methods for this class of filters.

and estimates for, the filter exponent B_u based on a variety of qualitative and quantitative observations. We summarize these constraints and estimates in Table 2. As previously mentioned, we the methods we follow to estimate the filter constants involve first estimating B_u (carried out in this section) followed by A_p (done in the next section). The various constraints discussed below serve different roles: some provide bounds, others provide point estimates, and others simply suggest approximate CF-invariance of the filter exponent.

Historical Estimates

The historically chosen value for B_u based on fitting the transfer function to the frequency response magnitude from simultaneous masking psychoacoustic experiments in humans is $B_{u,0} = 4$. The range of B_u deemed to be desirable historically based on the same simultaneous masking experiments is $3 \leq B_u \leq 5$ *. These are based on simultaneous masking experiments which were performed decades ago, and involve fitting to tuning curves.

If we are provided with a tuning curve - regardless of how it was measured, and we are only concerned with fitting to that tuning curve, then the most appropriate method of estimating filter constants is to fit to the tuning curve using classical filter design methods that take a frequency response magnitude over a length of frequencies and returns estimated filter constants. This is appropriate provided that individual data from the psychoacoustic tuning curves are reliable and not when we need to average over trials, subjects, or experiments or when recorded curves deviate from the shape of the

*Strictly, speaking it was the set of integers, $B_u \in \{3, 4, 5\}$ that were historically studied and found to be appropriate based on fitting to tuning curves from simultaneous masking experiment - often via Roex filter fits

filter classes. In these cases using characteristics-based methods are preferable to fitting.

More importantly, fitting to the tuning curve leaves us with a single set of filter constants specific to a certain case, and without intuition of how the constants relate to the filter behavior. Furthermore, reported data is often in the form of filter characteristics. In what follows we use focus on constraints and estimates of B_u that we can obtain based on filter characteristics. We focus on those observations relevant for designing auditory filters that mimic signal processing in the healthy human, but also arrive at conditions that apply regardless of species. Additionally, our analysis below more generally provide an example of how to use the characteristics-based design methods - given arbitrary specifications on filter characteristics or given reported specifications, present constraints based on observations, and identify which filter characteristics (including ratios) are most informative.

Conditions on the Variation of Filter Constants with CF

The first set of conditions we arrive at for B_u are with regards to its variation with respect to CF.

Trend in Quality Factor One such condition occurs due to the qualitative trend in reported quality factor. Our transfer functions are in normalized frequency, β , and we define our filter constants accordingly. We note that fixed values of A_p, b_p, B_u across filters in a filterbank result in the constant-Q filters (in other words, the bandwidth defined in f increases proportionally with CF). However, experimental observations suggest that the quality factor is larger for larger CF [Robles and

#	Data	B_u Condition/Value
N/A	condition on envelope of impulse response for half-integer domain	$\frac{3}{2} \leq B_u$
N/A	range of α (physiological, across lab species)	$3.86 \leq B_u$
$B_{u,0}$	historical (designed GTFs based on simultaneous masking psychophysical experiments in humans)	$B_u = 4$ (more generally, $B_u \in \{3, 4, 5\}$)
$B_{u,1}$	$g = g_1$ (chinchilla physiological data - specifically ANF WKS)	$B_u \approx 7.2$
$B_{u,2}$ for $CF > CF_{a b}$	$g = g_2$ (from r found to be species-invariant with that of humans from Q_{erb} from forward masking psychoacoustic experiments and human N_{sfoae} using the paradigm of Shera et al. (2010) ; and from the (conservative) range of η across species)	$2 \leq B_u$

Table 2. The table summarizes conditions on, and estimates of, the filter exponent based on historical extensions and based on reported values of characteristic ratios. Conditions regarding the approximate independence of B_u on CF are not mentioned in the table but are detailed in the main text.

[Ruggero \(2001\)](#); [Glasberg and Moore \(1990\)](#)]. Based on equation 5 and figure 2, this means that the value of A_p should be smaller for larger-CF filters and/or the value of B_u should be larger for larger-CF filters.

Condition from Traveling Wave Model The second set of observations are also regarding how we expect the filter constants to vary with CF. Let us return to the origin of GEFs and V which provided a unified framework for a filterbank and a single-partition box model of the cochlea. The model tied together the traveling wave and transfer function perspectives. As the energy inputted into the cochlea from the stapes is expected to predominantly travel in the forward direction (i.e. from the base to the apex). This translates to a requirement that the model constants parameterizing the wave number vary slowly with x ^{*} Consequently, we expect that the filter constants which parametrize the transfer functions - and which are the same as the model constants in this case, must vary slowly with CF.

Condition on Polarity A tighter condition on the variation of B_u with respect to CF comes from an observation regarding the polarity and zero crossing of auditory nerve fiber (ANF) click responses which were found to be the same across the length of the cochlea [[Guinan Jr \(2017\)](#)]. It is not clear why this occurs from a cochlear mechanism perspective as the value of B_u in the cochlear model is implicitly a function of material and geometric properties which *do* vary with x . Nevertheless, this observation provides a polarity condition on the oscillatory component of the impulse response of most filter classes. This is true for the sharp-filter approximation, GEFs, V filters, and P-GTFs but not for classical GTFs where the phase shift of the tonal component is not tied to B_u . Coupled with the above condition that the filter constants must vary slowly with CF translates into a condition that B_u is approximately constant with respect to CF. The approximate CF-independence of B_u also translates into approximately constant values for B_u -characteristic ratios - such as those in equation 6 and figure 3a, and further discussed in later sections. Because this condition is dependent on the filter class - or more specifically, on the filter exponent being tied to the phase shift of the tonal component of the impulse response as applied to the actual ANFs rather than filters we are attempting to

^{*}We note that this condition is most easily derived for another class of models - 1D two-way wave equations (such as those describing transmission line models) and is referred to as the WKB condition. Our cochlear model is a short-wave model collapsed from 2D into a one-way 1D wave equation which requires a separate derivation for the mathematical condition which is

design, we keep in mind that this condition may not necessarily hold. However, we later separately arrive at a condition on B_u from reported g that also suggests that B_u is CF-invariant, and hence we proceed with this conclusion.

Observations of Phase Accumulation The constant nature of B_u means that the phase accumulation is constant across CF. However, we currently do not have measurements of frequency response phase much away from the peak. Furthermore, the filter classes were constructed to fit responses primarily near the peak frequency and were not tested beyond it where the magnitude is negligible and data is not reliable. As a result, we do not give much credence to observations regarding phase accumulation with the exception of using the partial phase accumulated over the peak region which provides a lower bound for phase accumulation and hence for $\frac{B_u}{2}$.

Existing Reports of Variation The above conclusion that B_u is CF-invariant appears to contradict previous estimates of B_u for chinchilla reported in [Alkhairy and Shera \(2019\)](#). Those estimates were found by fitting \mathcal{V}_{CF} of equation 11 (which is related to GEFs and V filters but with an exponent of $B_u + 1$) to Wiener Kernel (WK) data from chinchilla ANFs. Specifically, [Alkhairy and Shera \(2019\)](#) showed that the trend lines for $B_u + 1$ ranged from about 4 for the lowest CF to about 6 for the highest CFs. However, we make the following notes about the previous findings: (1) there was a very large spread in estimated values of B_u from ANF WKS - from about 1.75 to 7.75 - this included a large spread in B_u estimated from WKS collected at the same CF from different chinchilla which implies that the trend lines alone provided insufficient information, (2) the ANF WK data included those that were very noisy at the peak, (3) while the sharp-filter approximation holds for the chinchilla base, it is not as reliable below a CF of 5 kHz in chinchilla, and (4) a lower bound on A_p was artificially imposed which affected the estimates for B_u . As a result, we build on the finding that B_u is approximately CF-invariant.

Constraint Due to Shape of Impulse Response Envelope

The shape of the envelope of the impulse response provides a lower bound on the value of B_u . The impulse or click responses in alive animals across species and CFs may roughly be described by a tone modulated by an envelope that grows at the earlier times then decays - rather than having a pure decay (we are not concerned with frequency glides or phenomenon of waxing and waning here). Based on the impulse response approximation for GEFs with integer and half-integer B_u (equation 9), this translates to a constraint, $B_u \geq \frac{3}{2}$ as $B_u = 1$ leads to an impulse response with a pure decay. This also applies to the other filter classes as their impulse responses can also be approximated by that of equation 9.

Constraints from Characteristic Ratios

The final type of constraints come from reported values and ranges of ratios of filter characteristics. The expressions for some of the B_u -dependent characteristic ratios (specifically α and g) were provided in equation 6.

Ratio of Quality Factors The first observation is regarding the ratio $\alpha \triangleq \frac{Q_{\text{erb}}}{Q_{10}}$ of equation 6. [Shera and Guinan Jr \(2003\)](#) found that $1.7 \leq \alpha \leq 1.8$ across species and CFs. Using $1.7 \leq \alpha \leq 1.8$ and based on equation 6, we arrive at a condition on the range of possible values for the filter exponent: $3.86 \leq B_u$. Figure 7 shows the dependence of B_u on α and illustrates that α in this range should only be used to provide a lower bound and cannot be used to reliably estimate a specific value of B_u .

Note that another possibility for the bounds on B_u may be inferred from $1.7 \leq \alpha \leq 1.8$. This other possibility is that $0.73 \leq B_u \leq 0.8$. However, this is inconsistent with the earlier minimum condition we imposed on B_u to guarantees a growth then decay in the envelope of the impulse response of GEFs, and also contradicts other observations detailed later in this paper.

Ratio of Quality Factor to Peak Group Delay Another characteristic ratio which we have reported data for and which provides a constraint on B_u is the ratio $g \triangleq \frac{Q_{\text{erb}}}{N_\beta}$ which was previously defined in equation 6. In the following discussion, we impose $b_p = 1$ so that g is purely a function of B_u . Reported values of g may provide constraints on (or estimates of) B_u . In figure 7, we show how B_u estimates vary with g . In what follows, we discuss two sets of observations related to g - which we refer to g_1 and g_2 , that lead to constraints on B_u .

First Estimate One reported value for g comes from [Shera et al. \(2010\)](#) who computed g as the ratio of Q_{erb} and N_β that were both computed from frequency response curves of ANF WKS at low SPLs in chinchilla. We refer to this estimate of g as g_1 which was reported to be $g_1 \approx 1.25 (\pm 0.02)$ along the length of the cochlea. Solving equation 6 for B_u (and taking the solution that

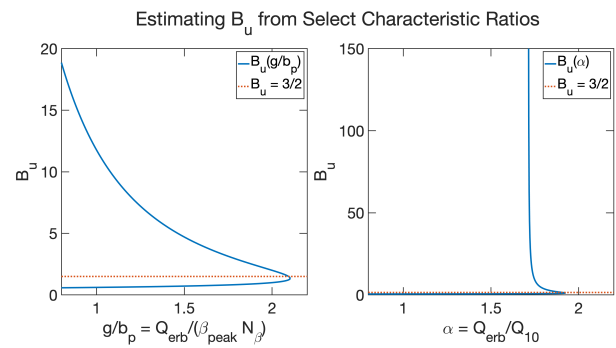


Figure 7. B_u is plotted (blue solid line) vs two characteristic ratios ($\frac{g}{b_p}$ and α). A line at $B_u = \frac{3}{2}$ is included (red dashed line) to indicate a lower limit on acceptable B_u . If we include this constraint, we may express B_u as a function of the filter characteristic ratios. We note that especially for $\alpha < 1.75$, there is little value in this reported characteristic ratio as far as estimating B_u . This is due to the fact that in this range, $|\frac{dB_u}{d\alpha}|$ is relatively large and hence small differences in reported values of α can result in wildly different values for B_u and hence we cannot arrive at credible estimates for B_u from α in this range. The same holds true for smaller values of $\frac{g}{b_p}$ (occurring at larger values of B_u) though to a lesser extent.

is greater than unity), we arrive at an approximately CF-invariant value of $B_{u,1} \approx 7.2$ from g_1 .

We note that we had previously computed an estimate of B_u from g_1 in [Alkhairy \(2024\)](#) using a more long-winded approach from a ratio $\nu \triangleq \frac{Q_{10}}{N_\beta} \equiv \frac{g_1}{\alpha}$. This was done because - at the time, we had derived expressions for N_β and Q_{10} but not for Q_{erb} . We had additionally reported B_u as the closest integer and arrived at $B_u = 7$. This is consistent with our current estimate for B_u from g_1 of $B_{u,1} \approx 7.2$. We later use this estimate of $B_{u,1}$ along with two sets of reported Q_{erb} to estimate the filter constant, A_p .

Second Estimate We may also obtain estimates for B_u using a second estimate of g which we refer to as g_2 . We compute this estimate for g as $g = r\eta$ from the tuning ratio, r , and a ratio, η .

The tuning ratio, r , was defined by [Shera et al. \(2010\)](#) as,

$$r \left(\frac{\text{CF}}{\text{CF}_{a|b}} \right) \triangleq \frac{Q_{\text{erb}}}{N_{\text{sfoae}}}, \quad (14)$$

where $\text{CF}_{a|b}$ is the CF at the apical-basal transition and N_{sfoae} is the normalized group delay of SFOAEs at a frequency corresponding to the CF of the filter of interest.

We define the ratio η as,

$$\eta \triangleq \frac{N_{\text{sfoae}}}{N_\beta}. \quad (15)$$

In what follows, we discuss reported values of r and η , then compute g as $g = r\eta$ to then provide an alternate condition for B_u based on these reported values.

The tuning ratio r has previously been reported across various species - including humans. The first reported value for r which we refer to as r_2 was computed

using $N_{\text{sfoae}} = N_{\text{sfoae, shera}}$ with SFOAEs gathered and processed as described in [Shera et al. \(2010\)](#). The Q_{erb} used to compute r_2 for most species was based on physiological experiments. In the case of humans, Q_{erb} was computed from noninvasive experiments. More specifically, it was based on a forward masking paradigm described in [Oxenham and Shera \(2003\)](#) to provide $Q_{\text{erb}} = Q_{\text{forw}}$. This study reported that the $r_2 \left(\frac{\text{CF}}{\text{CF}_{a|b}} \right)$ computed in this manner is approximately species-invariant.

From figure 9 of [Shera et al. \(2010\)](#) we obtain an estimate $0.8 \leq r_2 \left(\frac{\text{CF}}{\text{CF}_{a|b}} \right) \leq 1$ for $\frac{\text{CF}}{\text{CF}_{a|b}} > 1$. We note that other studies provide (or may be used to compute) values for r that appear rather inconsistent with the above estimates - e.g. [Bentzen et al. \(2011\)](#), [Lineton and Wildgoose \(2009\)](#), and [Schairer et al. \(2006\)](#). We expect that these differing estimates of r and any differences between humans and other species are largely due to differences in the paradigms for obtaining SFOAEs and psychoacoustic tuning curves. This leads to an important cautionary note when estimating the set of filter constants using values of r together with another filter characteristic (e.g. N_{sfoae} or Q_{erb}). In particular, we must ensure that the reported values used are consistent in terms of definitions and methodologies.

As for η , we note that while a tighter condition on η exists based on figure 7 of [Shera et al. \(2010\)](#), we use a relatively weak condition that $1 \leq \eta_2 \leq 2$ ^{*}. From r_2 and η_2 , we obtain a second estimate for g . Specifically, $0.8 \leq g_2 \leq 2$. Computing the range of B_u from equation 6 (and taking the values that are greater than unity), we arrive at an approximate condition $2 \leq B_{u,2} \leq 18.85$ for $\text{CF} > \text{CF}_{a|b}$. The upper bound is unreliable as B_u is very sensitive to small changes in the value of g in this region of parameters (in contrast to the region prescribed by g_1) and hence not included in Table 2 or used towards estimating the filter constant A_p .

Historical Value of Exponent For reference, here we discuss the consistency of the historically chosen values of B_u with reported (and computed) values or ranges of α and g . Consistency does not imply that the historical values of B_u provide the ‘correct’ solution, but rather that they are one of many possible consistent solutions.

Recall the the reported range of α is $1.7 \leq \alpha \leq 1.8$ which lead to a condition, $3.86 \leq B_u$. The historically chosen value for B_u in humans ($B_{u,0} = 4$) corresponds to $\alpha = 1.8$. The range of B_u deemed to be desirable historically based on the same simultaneous masking experiments ($3 \leq B_u \leq 5$) corresponds to $1.78 \leq \alpha \leq 1.82$.

We note that g_1 (based on physiological observations from chinchilla and expected to hold in humans) results in a value for $B_u = B_{u,1} = 7.2$ that is greater than the historically imposed value of $B_u = B_{u,0} = 4$ based on simultaneous masking psychoacoustic experiments for humans. On the other hand $B_{u,0}$ is within the wide range for $B_{u,2}$ prescribed by the species-invariant value of g_2 for $\text{CF} > \text{CF}_{a|b}$. The g corresponding to the

historical $B_{u,0} = 4$ has a value $g = g_0 = 1.6$, and B_u in the range historically found to be desirable, $3 \leq B_u \leq 5$ corresponds to $1.46 \leq g \leq 1.78$.

Estimates for Filter Pole

In the previous section, we used observations to estimate the value (or range of values) of the filter exponent B_u . Here, we provide estimates for the last filter constant, A_p , to be used for human auditory filterbanks given observations on some sets of filter characteristics (including characteristic-ratios). We then discuss limitations of our methods and estimates.

In choosing the set of observations used to estimate A_p (and before that, B_u), we bear in mind our application of interest, as well as the availability of reliable datasets, and the sensitivity of the estimates to the observed characteristics.

Following the methods described earlier, we first estimated b_p then B_u and finally estimate A_p . We set the peak frequency to occur at CF and hence set $b_p = 1$, and consider two estimates of B_u : $B_{u,0} = 4$ which is the historically used value based on fits to simultaneous masking curves, and $B_{u,1} = 7.2$ which was obtained from $g_1 = 1.25$ [†].

We then take each of these values of B_u along with reported values of Q_{erb} (shown in figure 9[‡]) to derive expressions for A_p as a function of CF as schematized in figure 8. In figure 10, we show the various resultant estimates for the filter constants for human auditory filters as a function of CF. In estimating A_p , we ensure that the quality factors used are consistent with the B_u . For example, to estimate A_p , we cannot combine quality factors obtained from forward masking experiments with estimated values for B_u obtained from fitting filters to tuning curves from simultaneous masking experiments. We note that unlike the case of $B_{u,0}$ which is tightly associated with Q_{sim} , we do not know what the appropriate choice of Q_{erb} is for $B_{u,1}$ based on g_1 . For this reason, we compute two estimates for $A_{p,1}$ using $B_{u,1}$ and two possible choices of Q_{erb} .

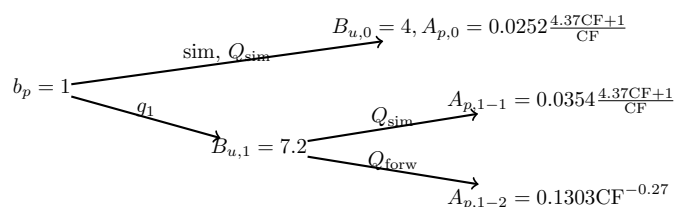


Figure 8. Process to arrive at estimated constants for human auditory filters as well as estimated values for the filter constants. CF is in kHz and the filter constants are dimensionless.

From Tuning Curves of Simultaneous Masking Experiments

For reference, we start by providing the value of A_p based on historical measurements. From equation 5 for Q_{erb} , and using the historical $B_u = B_{u,0} = 4$ we arrive at $A_p = A_{p,0} = \frac{1.0186}{Q_{\text{sim}}}$. This is consistent

^{*}We do this in consideration of unresolved questions regarding the deviation of this ratio from the value of 2 originally expected based on coherent reflection theory, and because these values found for chinchilla seem to differ from those previous reported for cats and guinea pigs [Shera and Guinan Jr \(2003\)](#)

[†]Which we assume to be species invariant and extrapolate to humans based on the arguments in [Shera and Guinan Jr \(2003\)](#); [Shera et al. \(2010\)](#)

[‡]Note that the reported values of Q_{erb} are over a particular CF, but we have extended this to a wider range of CFs for figure 10

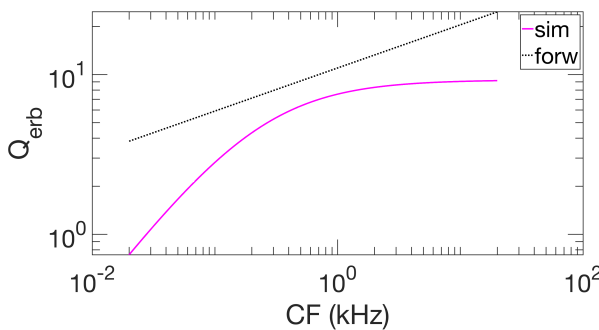


Figure 9. Reported values of Q_{erb} as a function of CF. We use the values of Q_{erb} to estimate the filter constant A_p given estimates of B_u and b_p . The Q_{erb} formulae used are based on simultaneous (magenta solid line) and forward masking paradigms (black dotted line). Both were extrapolated to cover the range of CF for humans.

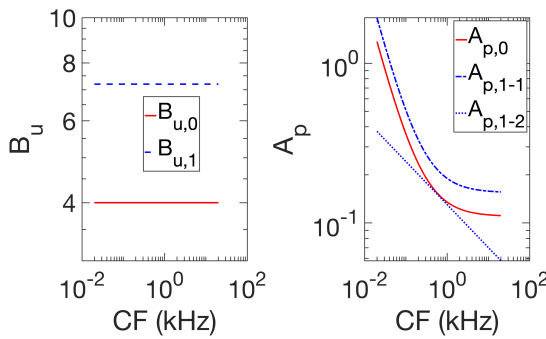


Figure 10. Estimated values for filter constants for filterbanks mimicking processing in humans. The estimates are based on a few reported sets of values for filter characteristics including characteristic ratios as detailed in the main text. For all these estimates, $b_p = 1$. In the left panel, estimate $B_{u,0}$ (red solid) is the historical choice, and the estimate $B_{u,1}$ (blue dashed) is obtained by extrapolating $g = g_1$ to humans. In the right panel, the estimate $A_{p,0}$ (red solid) is based on the historical Q_{sim} and $B_{u,0}$. The estimate $A_{p,1-1}$ (blue dash-dots) is computed from $B_{u,1}$ and Q_{sim} , and the estimate $A_{p,1-2}$ (blue dots) is computed from $B_{u,1}$ and Q_{forw} .

with the $b = 1.019(\text{ERB}_f)$ from Holdsworth et al. (1988) and Patterson et al. (1992). Together with the historical $Q_{\text{erb}} = Q_{\text{sim}}$ derived from the same tuning curves used to obtain $B_{u,0}$ historically, we arrive at $A_{p,0} = 0.0252 \frac{4.37\text{CF}+1}{\text{CF}}$ where the CF is in kHz. This is equivalent to what we would have gotten had we estimated A_p and B_u simultaneously by fitting to the historical tuning curves.

From g_1 and Q_{sim}

The next estimate for A_p in figure 10 comes from $B_{u,1}$ and reported values of Q_{erb} from simultaneous masking experiments, $Q_{\text{erb}} = Q_{\text{sim}} = \frac{10^3}{24.7} \frac{\text{CF}}{4.37\text{CF}+1}$ (with CF in kHz). Q_{sim} is reported based on tuning curves measured using simultaneous notched-noise masking psychoacoustic experiments performed in humans described in Glasberg and Moore (1990). This is the same set of experiments that were used to estimate the historical values for n and b of classical GTFs. Together with $B_u = B_{u,1}$, and based on the equation for Q_{erb} in

equation 5 (with $b_p = 1$), this results in an estimated $A_p = A_{p,1-1} = \frac{1.4334}{Q_{\text{sim}}} = 0.0354 \frac{4.37\text{CF}+1}{\text{CF}}$ where CF is in kHz.

From g_1 and Q_{forw}

The final estimate of A_p in figure 10 comes from $B_{u,1}$ coupled with $Q_{\text{erb}} = Q_{\text{forw}} = 11\text{CF}^{0.27}$ with CF in kHz is reported based on tuning curves measured using forward masking psychoacoustic experiments performed in humans for CFs between 1 and 8 kHz as described in Oxenham and Shera (2003). Together with $B_u = B_{u,1}$, and based on the equation for Q_{erb} in equation 5 (with $b_p = 1$), this results in an estimated $A_p = A_{p,1-2} = \frac{1.4334}{Q_{\text{forw}}} = 0.1303\text{CF}^{-0.27}$ where CF is in kHz but A_p is dimensionless.

Limitations

In what follows, we note various caveats in our estimates and limitations of our approach for estimating filter constants from reported characteristics as suitable for auditory filterbanks mimicking healthy human processing.

Assumptions Regarding Constants We note that all estimates and constraints are valid only in the regime where the sharp-filter approximation remains accurate, i.e., small A_p (as is the case for humans) and when dealing with peak-centric characteristics. The estimates and constraints also build on our conclusion that B_u is CF-invariant. However, due to some conflicting observations described earlier, it may be useful to assess the validity of this conclusion.

Distinguishing Classes In providing estimates for filter constants using reported values of characteristics, we were only concerned with estimates that hold across filter classes. We were not concerned with distinguishing which filter class is more appropriate. That would require an additional set of data and deriving additional expressions for distinguishing characteristics such as the asymmetry of the slope of the magnitude about the peak.

Uncertainty in Characteristics Regardless of whichever set of filter characteristics we use, we must be cognizant of the error inherent in recordings and reported values - e.g. due to noisiness and assumptions used to obtain values of reported characteristics from measurements. In previous sections, we have considered several cases where this may have an effect by studying the sensitivity of B_u estimates with respect to each of the characteristic ratios over the region of interest.

Extrapolating from Different Species In the case of humans, we face a dearth of reliable and accepted reported values of filter characteristics, which leads us to integrating information from different species. In contrast, this would not be the case for cats, for instance, where revcor data can be used to even calculate the most peak-centric magnitude characteristics such as S_β .

The g_1 used to estimate B_u is not only from a different species, but also depends on certain underlying

assumptions from the Wiener Kernel methods. Ideally, when estimating filter constants for humans, we would have preferred to use readily available data from humans - specifically group delays from SFOAEs, N_{sfoae} along with Q_{erb} from psychoacoustic tuning curves. However, this approach requires accurate and precise values for η to convert N_{sfoae} to N_β which we do not have *. This led us to using psychoacoustic Q_{erb} and g_1 extrapolated from WNs from chinchilla ANFs.

In general regardless of the filter characteristics used, when estimating filter constants from characteristics for the case of humans, we may need to extrapolate characteristics that are expected to be species or CF-invariant from different species and locations and may even arise from different types of experiments (e.g. ANF, mechanical, or psychoacoustic), and to integrate information from different stimulus levels or those which are of different nature - e.g. from frequency responses and threshold tuning curves - this is also the case if we could use N_{sfoae} with Q_{erb} to estimate the filter constants.

Masking Paradigms One other caveat to keep in mind is the effect of choices made for the psychoacoustic experiments from which we obtain Q_{erb} . We used Q_{erb} reported from psychoacoustic tuning curves using two specific forward and simultaneous masking paradigms as there is some debate regarding the appropriateness of various masker paradigms for estimating the frequency response magnitude. Additional experimental choices may also affect the reported values for Q_{erb} from psychoacoustic experiments such as masker duration especially at lower CFs [Lopez-Ramos et al. (2024)].

Alternative Methods Some of the advantages - and limitations, arise from our estimation of filter constants from filter characteristics. However, as previously mentioned, if we were solely interested in estimating one set of filter constants given a particular finely sampled and reliable tuning curve, then using our methods for estimating filter constants from filter characteristics is not the first choice. In this particular case, the most appropriate method is to use the gold standard of simultaneously estimating filter constants by fitting the filter frequency response magnitude to the psychoacoustic tuning curves.

Conclusions

Contributions

In this paper, we designed human auditory filters using recently reported values of filter characteristics in a manner that facilitates understanding how variations in those characteristics influence the estimated filter constants. Towards our goal, we explored the full degrees of freedom of the filter rather than fixing the value of constants to those historically estimated based on simultaneous masking experiments in humans. The filter characteristics we included are primarily those that are peak-centric. Specifically, we analyzed the dependence of filter characteristics on filter constants using a sharp filter approximation for the transfer function of three

*If we do have this information, we must be sure to use N_{sfoae} and η generated using the same experimental methods for obtaining SFOAEs using sagej.cls

classes of filters from the gammatone family. Our findings show that the choice of filter constants for auditory filters (e.g. the pole and filter exponent) greatly influence the behavior of auditory filters and ultimately the conclusions inferred from perceptual models as well as the performance of technologies that use auditory filterbanks.

Indeed, it is our belief that fully utilizing the degrees of freedom of any given filter class is more important and allows us to access more behavior than switching over to another filter class - unless we are interested in filter behavior that cannot fundamentally be achieved by a certain class of filters - e.g. as relates to power spectrum asymmetry or nonlinear behavior. Hence, revisiting the parameter space was both theoretically and practically essential.

We also derived expressions for characteristic ratios that depend on either B_u or A_p including ratios such as g for which we have reported values that we used to constrain the values of filter constants for a given species or application. We studied the sensitivity of the filter characteristics to filter constants which informed which set of characteristics may be reliably used to design filters based on. We developed improved methods to design filters given specifications on sets of filter characteristics, and then demonstrated the accuracy of our findings regarding filter behavior (and implicitly our design methods) as applied to three different classes of realizable linear filters when A_p is small (as is the case for humans across CF). Lastly, we used these methods to design human auditory filterbanks by using the constraints on B_u from reported observations and characteristic ratios along with reported values of Q_{erb} from both simultaneous and forward masking psychoacoustic experiments in humans.

Future Directions

Our expressions, constraints, and methods may further be used to directly and accurately design auditory filters if the native specifications provided are sets of filter characteristics. Additionally, these methods can be used to *systematically* investigate the dependence of perceptual and technological study outcomes on filter characteristics - e.g. by studying the dependence on isolated characteristics (by varying ERB while fixing maximum group delay, or varying the 10 dB quality factor while fixing downward convexity). This is motivated by studies reporting sensitivity based on (usually ad hoc) variation of certain parameters - e.g. ERB and filter exponent. The outcomes influenced by changing filter characteristics include: intelligibility scores of bandpass-filtered speech [Warren et al. (2004)], accuracy of speech recognition [Dimitriadis et al. (2010); Slaney and Seltzer (2014)], direction of arrival and sound source localization models [Dietz et al. (2011)], mutual information between articulatory gestures of vocal tracts and acoustic and perceptual features [Ghosh et al. (2011)], and accuracy of speech intelligibility models for cochlear implants [Cosentino et al. (2013)]. This work may also be used to understand the

cochlea's role in perception via underlying unified models [Alkhairy and Shera (2019)].

We note that our interest was not only to estimate the filter constants given a particular tuning curve - which lead to the filter characteristics-based approach. However, we encourage fitting the filters to the forward masking tuning curves and estimating the filter constants to check our estimates for humans based on these data. It is also useful to then compute g from the filter constants estimated in this way in order to check the validity of our extrapolation of g across species and CFs.

Our analyses and methods may be extended to include specifications on combined spectrotemporal characteristics as is relevant for studying certain perceptual functions [Moore (2008)]. Future work may include other investigation and derivation of methods including filter characteristics specific to certain filter classes (such as asymmetry), and using those characteristics for estimating filter constants. Measure of uncertainty may also be derived for the estimated filter constants based on our expressions for filter characteristics and can be used if we are provided with the standard deviation of reported characteristics.

We have tested the accuracy of our results and methods for three related classes of auditory filters from the gammatone family of filters and expect that our conclusions hold for other such classes in the same family as well, but it is appropriate to test for accuracy for those classes of filters if we are interested in designing filters of those classes - particularly if their shape is fundamentally different in the peak region or they have additional degrees of freedom that affect behavior in the peak region. Lastly, it is desirable to build on this work towards quasilinear filters and handling nonlinear versions of the filters as is especially relevant for hearing loss simulations [Irino and Patterson (2020)].

Appendix: Derivation of Expression for ERB in Terms of Filter Constants

Here we derive our expressions for ERB_β and its associated quality factor (in equation 5) in terms of the filter constants. The ERB_β (which we will refer to as ERB in this section for simplicity) is defined as follows for a filter with transfer function H :

$$\text{ERB} \triangleq \frac{1}{|H(\beta_{\text{peak}})|^2} \int_0^\infty |H(\beta)|^2 d\beta, \quad (16)$$

where H may be H_P, H_V, H_{GTF} , or the transfer function of any other bandpass filter. We note that when computing the ERB numerically, the lower limit of integration is replaced with a 'small-enough' value β_1 and the upper limit of integration is replaced with a 'large-enough' value β_2 .

Let us return to the definition of ERB in the above equation, substitute H by $G = H_{\text{sharp}}$ which approximates the transfer function of realizable filters of interest. This leads to,

$$\text{ERB} \approx \frac{1}{|G(\beta_{\text{peak}})|^2} \int_0^\infty |G(\beta)|^2 d\beta, \quad (17)$$

or equivalently,

$$\text{ERB} \approx \frac{1}{|G_{\text{max}}|^2} I_\infty, \quad (18)$$

with,

$$I_\infty = \int_{-\infty}^\infty |G(\beta)|^2 d\beta, \quad (19)$$

where we have replaced the lower limit of integration by $-\infty$ for simplicity. This is appropriate because $|G|$ (the magnitude of H_{sharp}) is negligible for $\beta < 0$ in the parameter region of interest.

From the expression for G (equation 4 and its magnitude - see Alkhairy (2025a)), we derive,

$$|G_{\text{max}}|^2 = A_p^{-2B_u}. \quad (20)$$

To derive our expression for I_∞ , we rewrite it as follows,

$$I_\infty = \lim_{n \rightarrow \infty} J(\beta) \Big|_{-n}^n, \quad (21)$$

with,

$$\begin{aligned} J(\beta) &= \int^\beta |G(\beta')|^2 d\beta' \\ &= \int^\beta \left((A_p^2 + (\beta' - b_p)^2)^{-B_u/2} \right)^2 d\beta' \\ &= \underbrace{\frac{\beta - b_p}{A_p^{2B_u}}}_{\triangleq \zeta} {}_2F_1\left(\frac{1}{2}, B_u; \frac{3}{2}; -\left(\frac{\beta - b_p}{A_p}\right)^2\right), \end{aligned} \quad (22)$$

This expression is in terms of the Gauss Hypergeometric Function (GHF), which - for the case of $|z| > 1$ ^{*}, is expressed as,

$$\begin{aligned} {}_2F_1(a, b; c; z) &= \frac{\Gamma(b-a)\Gamma(c)}{\Gamma(b)\Gamma(c-a)} (-z^{-1})^a {}_2F_1(a, a-c+1; a-b+1; z^{-1}) \\ &+ \frac{\Gamma(a-b)\Gamma(c)}{\Gamma(a)\Gamma(c-b)} (-z^{-1})^b {}_2F_1(b, b-c+1; -a+b+1; z^{-1}). \end{aligned} \quad (23)$$

To use equation (23) for equation (22) of the ERB, we define z and y as

$$z = -y = -\left(\frac{\beta - b_p}{A_p}\right)^2, \quad (24)$$

with $|\beta| \rightarrow \infty \implies z \rightarrow -\infty$, and with $a = \frac{1}{2}, b = B_u, c = \frac{3}{2}$, and $\Gamma(1/2) = \sqrt{\pi}, \Gamma(3/2) = \sqrt{\pi}/2, \Gamma(1) = 1$. As a result, we have,

$$\begin{aligned} {}_2F_1\left(\frac{1}{2}, B_u; \frac{3}{2}; -y\right) &= \frac{\Gamma(B_u - \frac{1}{2}) \frac{\sqrt{\pi}}{2}}{\Gamma(B_u) 1} y^{-\frac{1}{2}} {}_2F_1\left(\frac{1}{2}, 0; \frac{3}{2} - B_u; -y^{-1}\right) \\ &+ \frac{\Gamma(\frac{1}{2} - B_u) \frac{\sqrt{\pi}}{2}}{\sqrt{\pi} \Gamma(\frac{3}{2} - B_u)} y^{-B_u} {}_2F_1(B_u, B_u - \frac{1}{2}; B_u + \frac{1}{2}; -y^{-1}) \end{aligned} \quad (25)$$

The first GHF in the above expression is simply = 1 due to the zero argument. We expand the second term using the formula for GHF for $|z| < 1$,

$${}_2F_1(a, b; c; z) = 1 + \frac{ab}{c} z + O(z^2) \quad (26)$$

^{*}which is the relevant form of the GHF in our case taking $\beta \rightarrow \infty, -\infty$

and obtain,

$${}_2F_1\left(\frac{1}{2}, B_u; \frac{3}{2}; -y\right) = a_1 y^{-\frac{1}{2}} + a_2 y^{-B_u} \left(1 + B_u \frac{B_u - \frac{1}{2}}{B_u + \frac{1}{2}} (-y^{-1}) + O(y^{-2})\right), \quad (27)$$

with,

$$\begin{aligned} a_1 &= \frac{\sqrt{\pi}}{2} \frac{\Gamma(B_u - \frac{1}{2})}{\Gamma(B_u)} \\ a_2 &= \frac{1}{2} \frac{\Gamma(\frac{1}{2} - B_u)}{\Gamma(\frac{3}{2} - B_u)}. \end{aligned} \quad (28)$$

Substituting the above expansion for ${}_2F_1\left(\frac{1}{2}, B_u; \frac{3}{2}; -y\right)$ for large y into equation (22) for $J(\beta)$, we get,

$$\begin{aligned} J(\beta) &= \frac{\beta - b_p}{A_p^{2B_u}} a_1 y^{-\frac{1}{2}} \\ &+ a_2 y^{-B_u} \left(1 + B_u \frac{B_u - \frac{1}{2}}{B_u + \frac{1}{2}} (-y^{-1}) + O(y^{-2})\right). \end{aligned} \quad (29)$$

As $|\beta| \rightarrow \infty$, all but the first term go to zero due to $B_u > 1$. This results in,

$$\begin{aligned} \lim_{|\beta| \rightarrow \infty} J(\beta) &= \frac{\beta - b_p}{A_p^{2B_u}} a_1 y^{-\frac{1}{2}} \\ &= \frac{\beta - b_p}{A_p^{2B_u}} a_1 \left(\frac{\beta - b_p}{A_p}\right)^2)^{-\frac{1}{2}} \\ &= \frac{\beta - b_p}{A_p^{2B_u}} a_1 \frac{A_p}{|\beta - b_p|} \\ &= a_1 A_p^{1-2B_u} \frac{\beta - b_p}{|\beta - b_p|}. \end{aligned} \quad (30)$$

Therefore,

$$\lim_{\beta \rightarrow \infty} J(\beta) = a_1 A_p^{1-2B_u}, \quad (31)$$

and,

$$\lim_{\beta \rightarrow -\infty} J(\beta) = -a_1 A_p^{1-2B_u}, \quad (32)$$

which - by equation (21), result in,

$$I_\infty = 2a_1 A_p^{1-2B_u} = \sqrt{\pi} \frac{\Gamma(B_u - \frac{1}{2})}{\Gamma(B_u)} A_p^{1-2B_u}. \quad (33)$$

Consequently based on equation 18 and using equation 20, we arrive at,

$$\text{ERB}_\infty = \sqrt{\pi} \frac{\Gamma(B_u - \frac{1}{2})}{\Gamma(B_u)} A_p, \quad (34)$$

and its associated quality factor,

$$Q_{erb} = \frac{b_p}{\sqrt{\pi} A_p} \frac{\Gamma(B_u)}{\Gamma(B_u - \frac{1}{2})}, \quad (35)$$

as shown in equation 5.

We note that for positive integer values of B_u (and $b_p = 1$), the Q_{erb} we derived above based on H_{sharp} is very well approximated by the previously derived expression for GTFs, which we denote in the following equation as $Q_{erb,\text{GTF}}$. The expression for $Q_{erb,\text{GTF}}$ was found by deriving the ERB_f from the impulse response of the classical GTFs - by using Parseval's theorem as

described in Holdsworth et al. (1988) and detailed in Darling (1991).

$$\begin{aligned} Q_{erb,\text{GTF}} &= \frac{\text{CF}}{\text{ERB}_f} \\ &= \frac{\text{CF}}{\pi b} \frac{(n-1)!^2 2^{2n-2}}{(2n-2)!} \\ &= \frac{1}{\pi A_p} \frac{(n-1)!^2 2^{2n-2}}{(2n-2)!}. \end{aligned} \quad (36)$$

References

- S. A. Alkhairy. Cochlear wave propagation and dynamics in the human base and apex: Model-based estimates from noninvasive measurements. In *AIP Conference Proceedings*, volume 3062, page 020010. AIP Publishing LLC, 2024.
- S. A. Alkhairy. Characteristics-based design of generalized-exponent bandpass filters. *IEEE Access*, 2025a.
- S. A. Alkhairy. Rational-exponent filters with applications to generalized exponent filters. *IEEE Transactions on Circuits and Systems I: Regular Papers*, 2025b.
- S. A. Alkhairy and C. A. Shera. An analytic physically motivated model of the mammalian cochlea. *The Journal of the Acoustical Society of America*, 145(1):45–60, 2019.
- T. Bentsen, J. M. Harte, and T. Dau. Human cochlear tuning estimates from stimulus-frequency otoacoustic emissions. *The Journal of the Acoustical Society of America*, 129(6):3797–3807, 2011.
- S. Cosentino, T. H. Falk, D. McAlpine, and T. Marquardt. Cochlear implant filterbank design and optimization: A simulation study. *IEEE/ACM Transactions on Audio, Speech, and Language Processing*, 22(2):347–353, 2013.
- A. Darling. Properties and implementation of the gammatone filter: a tutorial. *Speech Hearing and Language, Work in Progress, University College London, Department of Phonetics and Linguistics*, pages 43–61, 1991.
- M. Dietz, S. D. Ewert, and V. Hohmann. Auditory model based direction estimation of concurrent speakers from binaural signals. *Speech Communication*, 53(5):592–605, 2011.
- D. Dimitriadis, P. Maragos, and A. Potamianos. On the effects of filterbank design and energy computation on robust speech recognition. *IEEE transactions on audio, speech, and language processing*, 19(6):1504–1516, 2010.
- P. K. Ghosh, L. M. Goldstein, and S. S. Narayanan. Processing speech signal using auditory-like filterbank provides least uncertainty about articulatory gestures. *The Journal of the Acoustical Society of America*, 129(6):4014–4022, 2011.
- B. R. Glasberg and B. C. Moore. Derivation of auditory filter shapes from notched-noise data. *Hearing research*, 47(1-2):103–138, 1990.
- J. J. Guinan Jr. Personal communication, 2017.
- J. Holdsworth, I. Nimmo-Smith, R. Patterson, and P. Rice. Implementing a gammatone filter bank. *Annex C of the SVOS Final Report: Part A: The Auditory Filterbank*, 1: 1–5, 1988.

T. Irino and R. D. Patterson. The gammachirp auditory filter and its application to speech perception. *Acoustical Science and Technology*, 41(1):99–107, 2020.

Y. Jin, H. Su, C. Xu, and Q. Guo. Application of gammatone filter bank to active noise control algorithm. In *2017 IEEE International Conference on Signal Processing, Communications and Computing (ICSPCC)*, pages 1–5. IEEE, 2017.

A. G. Katsiamis, E. M. Drakakis, and R. F. Lyon. Practical gammatone-like filters for auditory processing. *EURASIP Journal on Audio, Speech, and Music Processing*, 2007(1):063685, 2007.

B. Lineton and C. Wildgoose. Comparing two proposed measures of cochlear mechanical filter bandwidth based on stimulus frequency otoacoustic emissions. *The Journal of the Acoustical Society of America*, 125(3):1558–1566, 2009.

D. Lopez-Ramos, A. Eustaquio-Martin, L. E. Lopez-Bascuas, and E. A. Lopez-Poveda. Effect of stimulus duration on estimates of human cochlear tuning. *Hearing Research*, 451:109080, 2024.

Y. Matsumoto, M. Suzuki, H. Ogushi, and A. Omoto. Application of an auditory filter for the evaluation of sounds and sound fields. *Building Acoustics*, 18(1-2):175–188, 2011.

B. C. Moore. The role of temporal fine structure processing in pitch perception, masking, and speech perception for normal-hearing and hearing-impaired people. *Journal of the Association for Research in Otolaryngology*, 9(4):399–406, 2008.

A. J. Oxenham and C. A. Shera. Estimates of human cochlear tuning at low levels using forward and simultaneous masking. *Journal of the Association for Research in Otolaryngology*, 4(4):541–554, 2003.

R. D. Patterson, K. Robinson, J. Holdsworth, D. McKeown, C. Zhang, and M. Allerhand. Complex sounds and auditory images. In *Auditory physiology and perception*, pages 429–446. Elsevier, 1992.

L. Robles and M. A. Ruggero. Mechanics of the mammalian cochlea. *Physiological reviews*, 81(3):1305–1352, 2001.

K. S. Schairer, J. C. Ellison, D. Fitzpatrick, and D. H. Keefe. Use of stimulus-frequency otoacoustic emission latency and level to investigate cochlear mechanics in human ears. *The Journal of the Acoustical Society of America*, 120(2):901–914, 2006.

C. A. Shera and J. J. Guinan Jr. Stimulus-frequency-emission group delay: A test of coherent reflection filtering and a window on cochlear tuning. *The Journal of the Acoustical Society of America*, 113(5):2762–2772, 2003.

C. A. Shera, J. J. Guinan Jr, and A. J. Oxenham. Otoacoustic estimation of cochlear tuning: validation in the chinchilla. *Journal of the Association for Research in Otolaryngology*, 11(3):343–365, 2010.

M. Slaney and M. L. Seltzer. The influence of pitch and noise on the discriminability of filterbank features. In *INTERSPEECH*, volume 14, pages 2263–2267, 2014.

M. Slaney et al. An efficient implementation of the patterson-holdsworth auditory filter bank. *Apple Computer, Perception Group, Tech. Rep.*, 35(8):1–42, 1993.

Q. Tan and L. H. Carney. A phenomenological model for the responses of auditory-nerve fibers. ii. nonlinear tuning with a frequency glide. *The Journal of the Acoustical Society of America*, 114(4):2007–2020, 2003.

X. Valero and F. Alias. Gammatone cepstral coefficients: Biologically inspired features for non-speech audio classification. *IEEE transactions on multimedia*, 14(6):1684–1689, 2012.

R. M. Warren, J. A. Bashford Jr, and P. W. Lenz. Intelligibility of bandpass filtered speech: Steepness of slopes required to eliminate transition band contributions. *The Journal of the Acoustical Society of America*, 115(3):1292–1295, 2004.